https://doi.org/10.48048/tis.2024.7591

Steroid Compounds of *Manihot Esculenta* Crantz Var. Sao Pedro Petro (Tuber) and Their Cytotoxic Effects on Melanoma Cancer Cells (B16-F10)

Diana Widiastuti[1,*], Siti Warnasih[1], Ade Heri Mulyati[1], Sutanto[1], Eka Herlina[1], Triastinurmiatiningsih[2], Siska Elisahbet Sinaga[1], Supriatno Salam[3], Desi Harneti[4],Ronny Lesmana[5,6], Unang Supratman[4,6], Susianti[6], Dine Agustine[7] and Rahmaniar Mulyani[8]

[1]*Department of Chemistry, Faculty of Mathematics and Natural Science, Universitas Pakuan, Jawa Barat 16129, Indonesia*
[2]*Department of Biology, Faculty of Mathematics and Natural Science, Universitas Pakuan, Jawa Barat 16129, Indonesia*
[3]*Faculty of Pharmacy, Universitas Mulawarman, Kalimantan Timur 75119, Indonesia*
[4]*Department of Chemistry, Faculty of Mathematic and Natural Sciences, Universitas Padjadjaran, Jawa Barat 45363, Indonesia*
[5]*Department of Medicine, Faculty of Medicine, Universitas Padjadjaran, Jatinangor 45363, Indonesia*
[6]*Central Laboratory, Universitas Padjadjaran, Jatinangor 45363, Indonesia*
[7]*Department of Chemistry, Faculty of Mathematics and Natural Science, Syekh Yusuf Islamic University, Banten 15118, Indonesia*
[8]*Departement of Chemistry, Jenderal Achmad Yani University, Jawa Barat 40525, Indonesia*

([*]Corresponding author's e-mail: dianawidi25@unpak.ac.id)

Received: 10 October 2023, Revised: 21 October 2023, Accepted: 28 October 2023, Published: 20 February 2024

Abstract

The pharmacological research of *Manihot esculenta* has stated the potential present as an interesting cytotoxic activity caused by several compounds contained in this species. However, the research on Melanoma Malignant cells (B16-F10 cancer cells) has never been studied. In this study, the steroid compounds isolated from the tuber of Sao Pedro Petro (1 variety of species *M. esculenta* Crantz) were studied *in vitro* and further evaluated using the western blot technique. Three steroid compounds, namely β-sitosterol (1), Campesterol (2), and Cholesterol (3), were obtained from the *n*-hexane extract of fresh Cassava tubers (Manihot esculenta Crantz). The chemical structures of compounds 1 - 3 were determined through various spectroscopic techniques such as HR-TOFMS, and NMR (^{1}H, ^{13}C, DEPT 135 °, HMQC, HMBC, ^{1}H-^{1}H COSY), along with a comparison to previously reported spectral data. Additionally, the apoptotic signaling pathway was investigated using RT-qPCR and western blot analysis. Among the 3 compounds, Campesterol (2) exhibited the highest IC_{50} value and demonstrated significant inhibition of B16-F10 cell proliferation by inducing apoptosis through *caspase-3* activation. In conclusion, our study is the first to show that steroid compounds isolated from *M. esculenta* have activity against B16-F10 cells. This provides insight that steroids have the potential as chemopreventive agents to treat melanoma skin cancer.

Keywords: Apoptosis, *Manihot esculenta* Crantz, Melanoma, Steroids

Introduction

Manihot esculenta Crantz, a member of the spurge family, is the sole plant in its genus used for food in its native South America. It is often regarded as one of the largest sources of nutritional carbs for human consumption and is widely grown for industrial reasons in Brazil. Historical records indicate that cassava was introduced to various regions, including India, Java-Indonesia and the Philippines, during the late 18th century. The *M. esculenta* Cr. plant is abundant in a wide range of essential macronutrients and micronutrients. Additionally, it contains valuable antioxidants like à-carotene, as well as vitamins A and C, anthocyanins, steroids, saponins and glycosides [1-3]. Cassava can serve as both a nutritional food source and a therapeutic plant due to its nutrient makeup. It is often farmed as an annual crop in tropical and subtropical countries, largely for its starchy tuberous roots, which are an essential supply of carbohydrates [4,5].

In a study by Widiastuti *et al.* [6], *M. esculenta* C. has 99 varieties in Indonesia. They found that 47 varieties were safe for consumption, and the rest were not because they had a cyanogenic potential of more than 50 ppm. Based on data from Widiastuti *et al*. [7] they stated the cassava tubers that had CP above 50 ppm, namely Sao Pedro Petro from Cisarua, Bogor, where the results obtained had a cytotoxic effect on murine leukemia cancer cells P-388 with IC_{50} values for ethanol, *n*-hexane, ethyl extracts. Ethyl acetate and *n*-butanol, respectively, for 61.2, 15.8, 39.9 and 50.3 µg/m.

The earlier research documented the presence of flavonoid compounds in the leaves of *Manihot utilissima* Pohl. Among the flavonoids, quercetin-3-O-rutinoside, a member of the flavonoid group, was discovered in cassava root variety Sao Pedro Petro originating from Cisarua, Bogor. In addition to flavonoids, steroids were also detected in the roots of *M. esculenta*. [8]. One of the steroid compounds isolated by Sinaga *et al.* was stigmasterol, evaluated against MCF-7 Breast cancer, and classified as an inactive compound. Conversely, the previous research. reported 2 steroid compounds from the stem of *M. esculenta* C. These 2 compounds were tested for their biological activity against 4 bacteria, namely *Staphylococcus aureus*, *Streptococcus*, *Escherichia coli*, and *Pseudomonas aeruginosa*. The test results indicated that these 2 compounds did not have activity against all the tested bacterial cells [9].

Skin cancer, including both melanoma and non-melanoma, develops due to the abnormal growth of cells in skin tissue. It is the most frequently diagnosed cancer worldwide, particularly in areas with predominantly white populations, where the incidence rate is steadily increasing [10]. B16-F10 is a type of melanoma cell derived from murine C57BL/6 and is used as a human tumor model [11]. These cells are derived from the B16 cell line based on their ability to metastasize to the lungs after intravenous injection *in vivo* and then formed *in vitro* after 1 cycle (B16-F1) or 10 (B16-F10) [12,13]. B16-F10 is a cell subline that can metastasize to the lungs. As much as 40 % of B16-F10 cells are used in *in vivo* studies to study metastasis and solid tumor formation [14-16]. B16-F10 cells are resistant to interleukin (IL)-2 immunotherapy in high dose [17]. In addition, melanoma cells are known to resist chemotherapeutic agents doxorubicin and cisplatin [18].

One variety of the species *Manihot esculenta* Crantz is Sao Pedro Petro. This variety has not been extensively studied for the isolation of its compounds that play a role as skin cancer inhibitors. Therefore, this research aims to isolate these compounds and test their activity through the Induction of Apoptosis using the western blot method.

Materials and methods

Experimental section

Tools and materials

A Waters Xevo QTOF MS was used to capture mass spectra. NMR data were collected using a Jeol spectrometer at 500 MHz for ^{1}H and 125 MHz for ^{13}C, with TMS serving as the internal standard. Silica gel 60 was used for column chromatography. TLC plates were precoated with GF254 silica gel (Merck, 0.25 mm), and detection was achieved by spraying with a 10 % H2SO4 in Ethanol solution, followed by heating.

Isolation of compounds from Manihot esculenta Crantz

Cassava (*Manihot esculenta* Crantz) was cultivated in Cisarua, Bogor, West Java, Indonesia. The fresh cortex of cassava roots (5 kg) was subjected to exhaustive extraction with 49 L of ethanol at room temperature. After removing the solvent through vacuum evaporation, the resulting concentrated ethanol extract (340.01 g) was first mixed with water and then sequentially partitioned with *n*-hexane, ethyl acetate, and *n*-butanol. The evaporation of these fractions yielded crude extracts of *n*-hexane (10.90 g), ethyl acetate (25.18 g), and *n*-butanol (228.63 g), respectively.

The *n*-hexane fraction (10.90 g) was fractioned by vacuum liquid chromatography in silica gel 60 using gradient eluent of *n*-hexane, Ethyl acetate, and MeOH (10 %), according to TLC results obtained 8 fractions (A-H). Fraction B (1.2 g) was chromatographed on a column of silica gel and eluted with a gradient of *n*-hexane, Ethyl acetate, and MeOH (10 %) to give thirteen subfractions (B1-B7). Subsfraction B2 was combined (111.3 mg) and chromatographed on a column of silica gel, eluted with an isocratic eluent of *n*-hexane: Ethyl acetate (9:1), and obtained compound 3 (12.2 mg). Subsfraction B3 was combined (221.9 mg) and chromatographed on a column of silica gel, eluted with an isocratic eluent of *n*-hexane: Ethyl acetate (7:3) obtained compound 1 (22.2 mg). Subsfraction B3B was combined (47.6 mg) and chromatographed on a column of silica gel, eluted with an isocratic eluent of *n*-hexane: Ethyl acetate (8:2) obtained compound 2 (7.1 mg) [19,20].

B16-F10 Melanoma cell

B16-F10 cell was acquired from American Type Culture Collection (ATCC® CRL-6475™, Manassas, Virginia, USA). The medium used was Dulbecco's Modified Eagle's Medium (DMEM high glucose) (Cat. No. 11965118, Gibco, New York, USA) added with 10 % Fetal Bovine Serum (FBS) (Cat. No. 10082147, Gibco) and 1 % Penicillin-streptomycin (Cat. No. 15140112, Gibco). Cell incubation was conducted at 37 °C in a 5 % CO_2 incubator (Cat. No. 8000DH, Thermo Fisher Scientific, Waltham, Massachusetts, USA).

Antiproliferation assay

B16-F10 melanoma cells were seeded at a density of 1.7×104 cells per well in 96-well microplates (Cat. No. 701001, Nest, Jiangsu, China) and allowed to incubate for 24 h. Subsequently, the cells were exposed to different concentrations (1,000; 500; 250; 125; 62.50; 31.25; 15.63; 7.81 µg/mL) of *M. esculenta* ethanol extract, *n*-hexane fraction, ethyl acetate fraction, and *n*-butanol fraction. Cisplatin (Cat. No. C2210000, EDQM, Strasbourg, France) at a concentration of 42.97 µg/mL was used as a positive control, while 2 % DMSO (Cat. No. 102952, Merck Millipore, Massachusetts, USA) was used as the solvent control. DMEM was used as the media control, and untreated cells in DMEM were included as a control group. The cells were incubated for 48 h, and then Presto blue reagent (Cat. No. A13261, Thermo Fisher Scientific) was added to each well. Following a 2-hour incubation, absorbance at 570 and 600 nm was measured with a multimode reader (Cat. No. M200 Pro, Tecan, Männedorf, Switzerland). Following that, cell viability and IC_{50} values were computed [21,22].

Western blot B16-F10

Melanoma cells were cultured in a 24-well microplate (Cat. No. 702001, Nest) at a density of 1.0×105 cells per well for a duration of 24 h. Following this, the cells were subjected to treatment using an ethyl acetate fraction derived from *M. esculenta*, with concentrations varying at 125; 62.50; 31.25; 15.63 µg/mL, and cisplatin at 42.97 µg/mL serving as the positive control. The incubation period lasted for 10 h. Subsequently, the cells were collected and processed *in vitro*. A lysis buffer of 100 µL per well was added, comprising a mixture of RIPA and sample buffer in a 1:1 ratio, along with protein inhibitor and DTT (Cat. No. V3151, Sigma Aldrich).

The samples were heated at 96 °C for 5 min before being quickly frozen in a deep freezer for 2 - 3 min. SDS-PAGE (Cat. No. A25977, Thermo Fisher Scientific) was used to separate 10 µL of the lysate protein for 120 min. The SDS-PAGE gel was then transferred to a nitrocellulose membrane (Cat. No. 10600002, GE Healthcare, Illinois, USA) with a pore size of 0.45 µm using blotting equipment (Cat. No. B1000, Thermo Fisher Scientific) for 30 min. The membrane was then rinsed with Phosphate Buffer Saline Tween-20 0.1 % (PBST) (Cat. No. 18912014, Gibco) and incubated for 30 min with a blocking solution containing 0.25 % BSA.

The immunoblotting procedure on the membrane involved the use of primary antibodies targeting caspase-3 (Cat. No. #14220, Cell Signaling, Massachusetts, USA) at a dilution of 1:300, followed by an overnight incubation at 4 °C. Subsequently, the membrane was subjected to 3 washes with 0.1 % PBST, and appropriate secondary antibodies (anti-rabbit, Cat. No. C90501-02, Li-Cor, Nebraska, USA) were applied at a dilution of 1:10,000. Protein detection on the membrane was performed using the LICOR Odyssey system (CLx Imaging System, Li-Cor, Nebraska, USA). Image J software from the National Institutes of Health (NIH) in Bethesda, Maryland, USA was used to determine the thickness of the protein band. After stripping the membranes, they were incubated with Glyceraldehyde-3-Phosphate Dehydrogenase (GAPDH) (Cat. No. AF5718-SP, RnD System, Minnesota, USA) as an internal control [23-25].

Results and discussion

The results of compound isolation

The cortex of fresh cassava roots from *Manihot esculenta* Crantz was finely ground and subjected to sequential extraction using ethanol. The resulting extract was then partitioned into fractions using *n*-hexane, ethyl acetate, and *n*-butanol. The *n*-hexane fraction was further purified using column chromatography with silica gel 60, employing a gradient elution method. The obtained fractions were subjected to multiple rounds of normal-phase column chromatography to isolate steroid compounds [1-3].

- *β*-Sitosterol (1). White solid; ^{1}H-NMR ($CDCl_3$, 500 MHz) See **Table 1**; ^{13}C-NMR ($CDCl_3$, 150 MHz), see **Table 1**; HRTOF-MS (positive ion) m/z 415.3744 $[M+H]^+$, (calculated $C_{29}H_{50}O^+$, m/z 415.3790)

- Campesterol (2). White waxy solid; ^{1}H-NMR ($CDCl_3$, 500 MHz) see **Table 1**; ^{13}C-NMR ($CDCl_3$, 150 MHz), see **Table 1**. HRTOF-MS (positive ion) m/z 401.3744 $[M+H]^+$, (calculated $C_{29}H_{50}O^+$, m/z 401.3790)
- Cholesterol (3). White solid; ^{1}H-NMR ($CDCl_3$, 500 MHz) See table 1; ^{13}C-NMR ($CDCl_3$, 150 MHz), see **Table 1**; HRTOF-MS (positive ion) m/z 387.3669 $[M+H]^+$, (calculated $C_{27}H_{46}O^+$, m/z 387.7141).

The results of compound isolation

Elucidation of compound 1

Compound 1 was obtained as a white solid. The mass result of compound 1 should be 415.3744 $[M+H]^+$, (calculated 415.3790). The ^{1}H-NMR ($CDCl_3$ 500 MHz) spectrum of 1 showed the presence of 6 methyl proton sp^3 at δ_H 0.68 (3H, s, H-18), 0.79 (3H, d, H-27), 0.82 (3H, d, H-26), 0.83 (3H, t, H-29), 0.99 (3H, d, H-21) and 1.01 (3H, s, H-19) that was indicative of the presence of sitosterol groups [26], 11 methylene proton sp^3 at δ_H 1.04; 1.35 (2H, H-22), 1.13; 1.61 (2H, H-15), 1.18; 1.89 (2H, H-1), 1.19; 2.03 (2H, H-12), 1.20 (2H, H-23), 1.27 (2H, H-28), 1.35; 1.86 (2H, H-16),1.51 (2H, H-11), 1.85; 1.56 (2H, H-2), 1.53 (2H, H-7), 2.28 (2H, H-4), and also 7 methine proton sp^3 at δ_H 0.97 (1H, H-24), 0.98 (1H, H-9), 1.00 (1H, H-14), 1.10 (1H, H-17), 1.37 (1H, H-20), 1.70 (1H, H-25), 1.93 (1H, H-8), 1 oxygenated methine proton at δ_H 3.53 (1H, *m*, H-3), and 1 olefinic methine at δ_H 5.35 (1H, *d*, H-6).

The ^{13}C and DEPT 135° NMR spectrum of compound 1 showed the presence of 6 methyl carbons sp^3 at δc 12.0 (C-29), 12.1 (C-18), 18.9 (C-21), 19.5 (C-19), 20.0 (C-26), and 29.1 (C-27), 11 methylene carbon sp^3 at δc 21.2 (C-11), 23.2 (C-28), 24.4 (C-15), 26.1 (C-23), 28.4 (C-16), 31.8 (C-2), 32.0 (C-7),34.0 (C-22), 37.4 (C-1), 39.9 (C-12), 42.4 (C-4). Seven methine carbons sp^3 at δc 29.2 (C-25), 31.9 (C-8), 36.3 (C-20), 42.5 (C-24), 50.2 (C-9), 56.1 (C-17), 56.9 (C-14), 1 oxygenated methine carbon at δc 71.9 (C-3), 1 olefinic methine carbon at δc 121.9 (C-6), 2 quarternary carbons sp^3 at δc 36.6 (C-10), 45.8 (C-13) and 1 carbon olefinic quarter at δc 140.9 (C-5). The HMBC correlation of 1 showed that proton 6 at δ_H 5.35 ppm correlated to C-7 (δ_c 32.0 ppm); C-8 (δ_c 32.0 ppm); C-10 (δ_c 36.6 ppm) and C-4 (δ_c 42.4 ppm), proton 21 at 0.99 ppm correlate to C-17 (δ_c 56.1 ppm); C-20 (δ_c 36.3 ppm) and C-22 (δ_c 34.0 ppm), proton 29 at 0.83 ppm correlate to C-28 (δ_c 23.2 ppm). The cross peak of ^{1}H-^{1}H-COSY spectra observed that H2/H3/H4 indicates that the hydroxy group at C-3 and H6/H7/H8 indicate a double bond at C5/C6. Compound 1 agreed well with data from the literature [27], identified as *β*-sitosterol and can be seen in **Figure 1**.

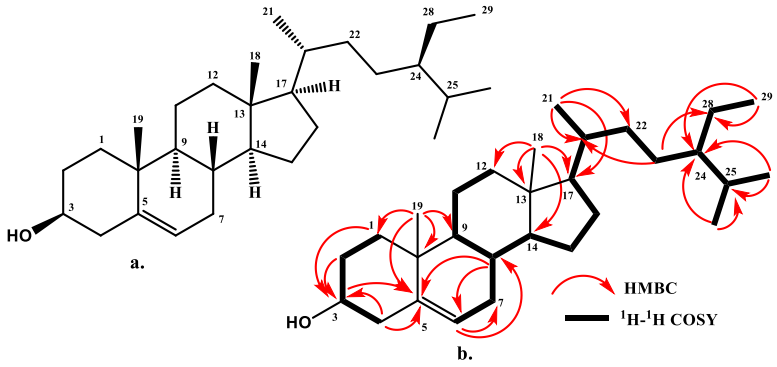

Figure 1 (a) Structure of *β*-Sitosterol (1) and (b). Selected COSY and HMBC correlations of *β*-Sitosterol (1).

Elucidation of compound 2

Compound 2 was obtained as a white waxy solid. The mass result of compound 2 should be 401.3744 $[M+H]^+$, (calculated 401.3790). The ^{1}H-NMR ($CDCl_3$ 500 MHz) spectrum of compound 2 showed the presence of 6 methyl protons sp^3 at δ_H 0.68 (3H, s, H-18), 0.85 (3H, t, H-28), 0.82 (3H, d, H-27), 0.84 (3H, d, H-26), 0.92 (3H, d, H-21) and 1.00 (3H, s, H-19), 10 methylene proton sp^3 at δ_H 1.04; 1.35 (2H, H-22), 1.13; 1.61 (2H, H-15), 1.15; 1.89 (2H, H-1), 1.19; 2.03 (2H, H-12), 1.20 (2H, H-23), 1.35; 1.86 (2H, H-16), 1.51 (2H, H-11),1.53 (2H, H-7), 1.85; 1.56 (2H, H-2), 2.28 (2H, H-4) and also 7 methine proton sp^3 at δ_H 0.97 (1H, H-24), 0.98 (1H, H-9), 1.00 (1H, H-14),1.10 (1H, H-17), 1.37 (1H, H-20), 1.70 (1H, H-25), 1.93 (1H, H-8), 1 oxygenated methine proton at δ_H 3.53 (1H, *m*, H-3), and 1 olefinic methine at δ_H 5.34 (1H, *d*, H-6).

The ^{13}C and DEPT 135 ° NMR spectrum of compound 2 showed the presence of 6 methyl carbon sp^3 at δ_C 11.9 (C-18), 18.8 (C-21), 19.4 (C-26, C-19), 22.6 (C-27), 22.8 (C-28), 10 methylene carbons sp^3 at δc 21.1 (C-11), 24.3 (C-15), 23.9 (C-23), 28.3 (C-16), 31.7 (C-2), 31.9 (C-7), 34.0 (C-22), 37.3 (C-1), 39.5 (C-12) and 42.3 (C-4), 7 methine carbon sp^3 at δc 28.1 (C-25), 31.9 (C-8), 36.3 (C-20), 39.4 (C-24), 50.1 (C-9), 56.2 (C-17), 56.8 (C-14), 1 oxygenated methine carbon at δc 71.9 (C-3), 1 olefinic methine carbon at δc 121.8 (C-6), 2 quarternary carbon sp^3 at δc 36.6 (C-10), 42.3 (C-13) and 1 carbon olefinic quarter at δc 140.8 (C-5). Compound 2 agreed well with data from the literature [27], identified as campesterol and this compound can be seen in **Figure 2**.

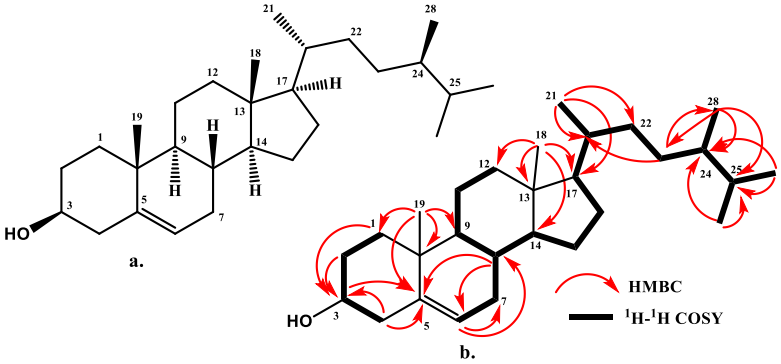

Figure 2 (a) Structure of Campesterol (2) and (b) Selected COSY and HMBC correlations of Campesterol (2).

Elucidation of compound 3

Compound 3 was obtained as a white solid. The mass result of compound 3 should be 387.3669 $[M+H]^+$, (calculated 387.7141). The ^{1}H-NMR ($CDCl_3$ 500 MHz) spectrum of compound 3 showed the presence of 5 methyl protons sp^3 at δ_H 0.66 (3H, s, H-18), 0.83 (3H, d, H-27), 0.85 (3H, d, H-26), 0.90 (3H, d, H-21) and 0.99 (3H, s, H-19), 11 methylene protons sp^3 at δ_H 0.94 (2H, m), 1.06; 1.32 (2H, H-22), 1.13; 1.77 (2H, H-15), 1.15; 1.83 (2H, H-1), 1.16; 2.00 (2H, H-12), 1.25 (2H, H-23), 1.35; 1.85 (2H, H-16), 1.51 (2H, H-11), 1.58 (2H, H-7), 1.81; 1.56 (2H, H-2), 2.28 (2H, H-4), and also 6 methine protons sp^3 at δ_H 0.97 (1H, H-9), 1.04 (1H, H-14),1.10 (1H, H-17), 1.36 (1H, H-20), 1.80 (1H, H-25), 1.93 (1H, H-8), 1 oxygenated methine proton at δ_H 3.53 (1H, *m*, H-3), and 1 olefinic methine at δ_H 5.34 (1H, *d*, H-6).

The ^{13}C-NMR spectrum of compound 3 displayed the presence of various carbon types. It exhibited 5 sp^3 methyl carbons at δ_C 11.9 (C-18), 18.8 (C-21), 19.5 (C-19), 22.6 (C-26), and 22.9 (C-27). Additionally, there were 11 sp^3 methylene carbons at δc 21.2 (C-11), 23.9 (C-23), 24.4 (C-15), 28.3 (C-16), 31.7 (C-2), 31.9 (C-7), 35.9 (C-22), 37.3 (C-1), 39.6 (C-24), 39.9 (C-12), and 42.4 (C-4). Furthermore, 6 sp^3 methine carbons were observed at δc 28.1 (C-25), 31.9 (C-8), 36.2 (C-20), 50.2 (C-9), 56.2 (C-17), and 56.9 (C-14). The spectrum indicated the presence of 1 oxygenated methine carbon at δc 71.9 (C-3) and 1 olefinic methine carbon at δc 121.8 (C-6). There were 2 sp3 quarternary carbons at δc 36.6 (C-10) and 42.4 (C-13), along with 1 olefinic quartet carbon at δc 140.8 (C-5). Compound 3 agreed well with data from the literature [27], identified as cholesterol and this compound can be seen in **Figure 3**.

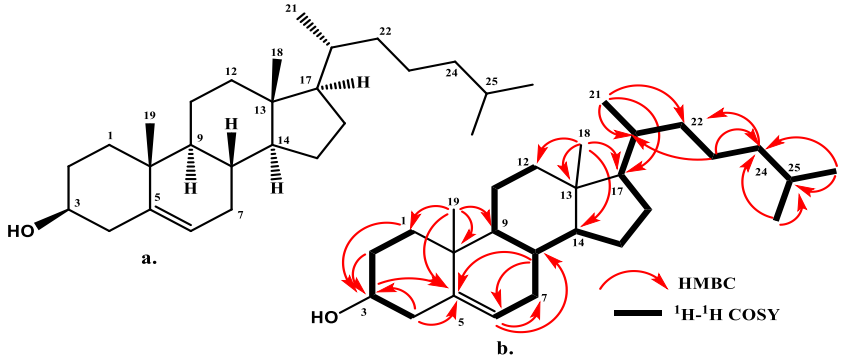

Figure 3 (a) Structure of Cholesterol (3) and (b) Selected COSY and HMBC correlations of Cholesterol (3).

A comparison of the results of the 3 compounds is summarized in **Table 1**.

The bioactivity of steroid compounds

In the initial stage, cytotoxic testing of compounds 1 - 3 was carried out on HeLa cells for 48 h, which showed cytotoxic activity, namely campesterol compound 2 with an IC_{50} value of 234 µg/mL, while other compounds showed an IC_{50} value of > 500 µg/mL. Sureshkumar *et al.* analyzed in silico 8 compounds, sterol group, from the plant *Calotropis gigantea*, where one of these compounds was campesterol [28]. The results of the docking analysis showed that campesterol had maximum potential against HPV16 oncoprotein E6 cervical cells, but there has been no further research into this *in vitro*, so this study was carried out with *in vitro* cytotoxic activity test of campesterol on skin Melanoma B16-F10 cells [29,30]. Based on the category of cytotoxic compounds according to Saini *et al.*, campesterol was toxic to Melanoma B16-F10 cancer cells (IC_{50} 160.4 µg/mL), less toxic to MCF-7 breast cancer cells (IC_{50} 276.2 µg/mL) and oral cavity Cal 27 (IC_{50} 314.9 µg/mL), and not toxic to A549 lung cells (IC_{50} > 500 µg/mL). Campesterol was able to inhibit the proliferation of B16-F10 cells, as indicated by its IC_{50} value of 160.4 µg/mL. An IC_{50} value represented the concentration at which a substance inhibited the growth of cells by 50 %. In this case, campesterol's IC_{50} value was greater than that of cisplatin (42.2 µg/mL), which suggested that campesterol was less potent than cisplatin in inhibiting cell proliferation. The analysis of cell viability was carried out, and the results showed that when B16-F10 cells were treated with campesterol, their cell viability decreased by more than 50 % compared to untreated cells. This was supported by noticeable alterations in cell morphology compared to the control group. Morphological cell changes included alterations in cell shape, size, and other visible characteristics. In this case, campesterol's cytotoxic activity was considered moderate, while cisplatin served as the positive control with higher cytotoxic activity [31,32] (**Figure 4**).

Table 1 NMR data (500 MHz for ^{1}H and 125 MHz for ^{13}C, in $CDCl_3$) for 1 - 3.

Position	1		2		3	
	^{13}C NMR δ_C	**^{1}H NMR δ_H (Σ H mult, J = Hz)**	**^{13}C NMR δ_C**	**^{1}H NMR δ_H (Σ H mult, J = Hz)**	**^{13}C NMR δ_C**	**^{1}H NMR δ_H (Σ H mult, J = Hz)**
1	37.2	1.18 (1H, m); 1.89 (1H, m)	37.3	1.15 (1H, m); 1.89 (1H, m)	37.3	1.15 (1H,m); 1.83 (1H,m)
2	31.6	1.85 (1H, m); 1.56 (1H, m)	31.7	1.85 (1H, m); 1.56 (1H, m)	31.7	1.81 (1H,m); 1.56 (1H,m)
3	71.8	3.53 (1H, m)	71.9	3.53 (1H, m)	71.9	3.53 (1H,m)
4	42.4	2.28 (2H, m)	42.3	2.28 (2H, m)	42.4	2.28 (2H,m)
5	140.9	-	140.8	-	140.8	-
6	121.9	5.35 (1H, d, 3.5)	121.8	5.34 (1H, br d, 5.0)	121.8	5.34 (1H, brd, 5.5)
7	32.0	1,53 (2H,m)	31.9	1.53 (2H, m)	31.9	1.58 (2H,m)
8	32.0	1.93 (1H, m)	31.9	1.93 (1H, m)	31.9	1.93 (1H,m)
9	50.2	0.98 (1H, m)	50.1	0.98 (1H, m)	50.2	0.97 (1H,m)
10	36.6	-	36.6	-	36.6	-
11	21.1	1.51 (2H, m)	21.1	1.51 (2H, m)	21.2	1.51 (2H,m)
12	39.9	1.19 (1H, m); 2.03 (1H, m)	39.5	1.19 (1H, m); 2.03 (1H, m)	39.9	1.16 (1H,m); 2.00 (1H,m)
13	45.8	-	42.3	-	42.4	-
14	56.9	1.00 (1H, m)	56.8	1.00 (1H, m)	56.9	1.04 (1H,m)
15	24.4	1.13 (1H, m); 1.61 (1H, m)	24.3	1.13 (1H, m); 1.61 (1H, m)	24.4	1,13 (1H,m); 1,77 (1H,m)
16	28.4	1.35 (1H, m); 1.86 (1H, m)	28.3	1.35 (1H, m); 1.86 (1H, m)	28.3	1.35 (1H,m); 1.85 (1H,m)
17	56.1	1.10 (1H, m)	56.2	1.10 (1H, m)	56.2	1.10 (1H, m)
18	12.1	0.68 (3H, s)	11.9	0.68 (3H, s)	11.9	0.66 (3H, s)
19	19.5	1.01 (3H, s)	19.4	1.00 (3H, s)	19.5	0.99 (3H, s)

Position	1		2		3	
	^{13}C NMR δ_C	**^{1}H NMR δ_H (Σ H mult, J = Hz)**	**^{13}C NMR δ_C**	**^{1}H NMR δ_H (Σ H mult, J = Hz)**	**^{13}C NMR δ_C**	**^{1}H NMR δ_H (Σ H mult, J = Hz)**
20	36.3	1.37 (1H, m)	36.3	1.37 (1H, m)	36.2	1.36 (1H,m)
21	18.9	0.99 (3H, d, 6.0)	18,8	0.92 (3H, d, 7.0)	18.8	0.90 (3H, d, 6,5)
22	34.0	1.04 (1H, m); 1.35 (1H, m)	34.0	1.04 (1H, m); 1.35 (1H, m)	35.9	1.06 (1H, m); 1.32 (1H,m)
23	26.1	1.20 (2H, m)	23,9	1.20 (2H, m)	23.9	1.25 (2H,m)
24	42.5	0.97 (1H, m)	39.4	0.97 (1H, m)	39.6	0.94 (2H,m)
25	29.2	1.70 (1H, m)	28.1	1.70 (1H, m)	28.1	1.80 (1H, m)
26	20.0	0.82 (3H d, 4.0)	19,4	0.84 (3H, d, 7.0)	22.6	0.85 (3H, d, 2.5)
27	19.1	0.79 (3H, d, 6.0)	22,6	0.82 (3H, d, 7.0)	22.9	0,83 (3H, d, 2.5)
28	23.2	1.27 (2H, m)	22,8	0.85 (3H, t, 7.0)	-	-
29	12.0	0.83 (3H, t)	-	-	-	-

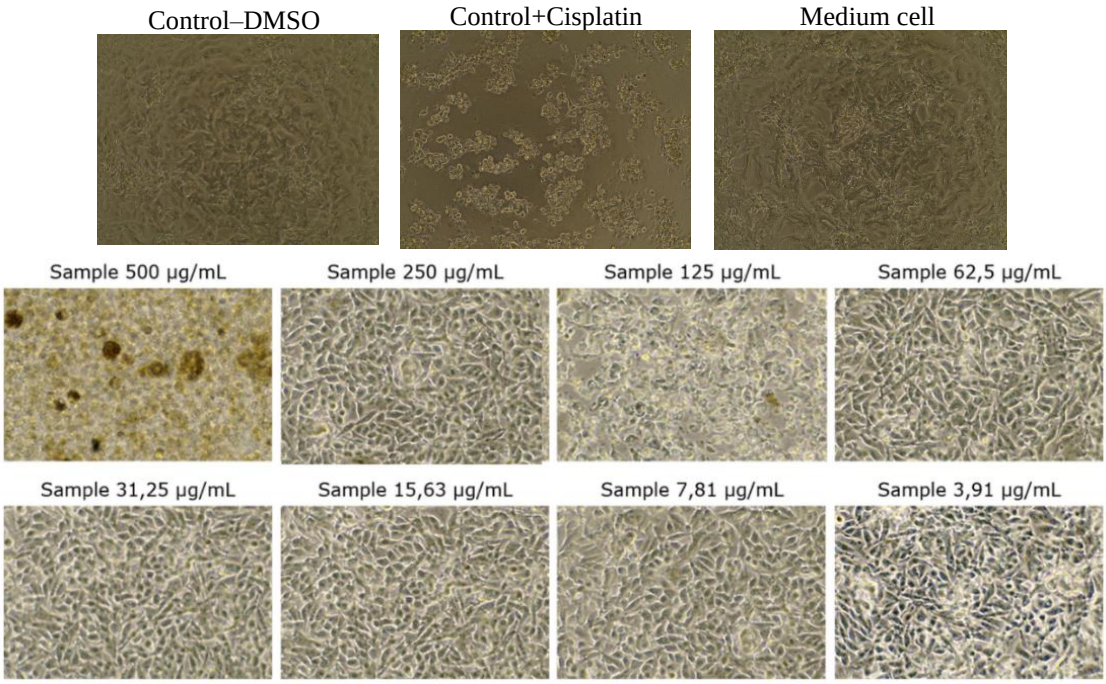

Figure 4 Changes in melanoma cell morphology (B16F10) treated with campesterol.

The results of the campesterol cytotoxic test on several types of cells showed the most significant cell proliferation inhibition activity against melanoma skin cancer cells (B16-F10). Hence, additional investigations were conducted to elucidate the molecular mechanism responsible for the cytotoxic impact of campesterol on B16-F10 melanoma cells. Apoptosis, a programmed form of cell death, can be activated by both internal and external signals [33,34]. Apoptosis comprised 2 primary signaling pathways: the extrinsic pathway and the intrinsic pathway. The intrinsic apoptotic pathway was primarily involved in the anticancer effects observed in this study [35-37]. One of the signaling of apoptosis was through caspase by activating caspase-9 and caspase-3, where caspase-9 was activated and induced by the apoptosome, then processes downstream caspases, such as caspase-3 to carry out the apoptotic process [38-40].

Caspase-9 and caspase-3 gene expression

The molecular mechanism of campesterol-induced apoptosis was examined by assessing apoptosis-related changes at the gene expression (mRNA) level. Cells were treated with a dose of ½ IC_{50}, then compared with positive controls of cisplatin and GAPDH as internal controls. RT-qPCR results showed that campesterol could inhibit the growth of B16-F10 melanoma cells and experienced an increase in caspase-3 expression by 2.5 times and caspase-9 by 1.3 times, while cells treated with cisplatin control experienced an increase in caspase-3 expression by 2.6 times and caspase-9 1.9 times when compared to controls. This demonstrated the involvement of caspase in campesterol-induced apoptosis, which occured intrinsically as a result of campesterol treatment in B16-F10 melanoma cells (**Figure 5**).

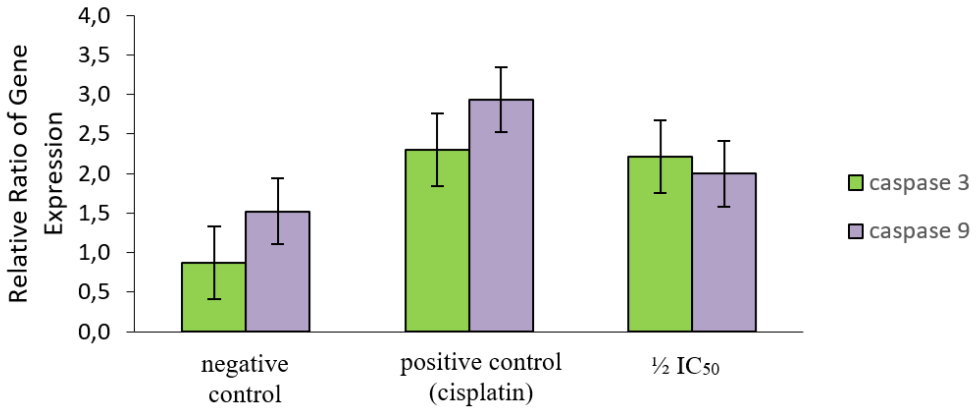

Figure 5 Relative ratio of caspase-3 and caspase-9 gene expression in campesterol-induced B16-F10 melanoma cells.

Expression of caspase-9 and caspase-3 proteins

After it was known that the death of B16-F10 melanoma cells treated with campesterol occurred through the process of inducing apoptosis from the mRNA level, then western blot testing was carried out on cells that had been treated. The work was carried out with 3 repetitions, where code 1 was internal control, code 2 was positive control, code 3 was ½ dose from IC_{50} and code 4 was the same as IC_{50} (160.4 µg/mL).

The western blot analysis results demonstrated an elevation in the expression levels of several pro-apoptotic proteins, specifically cleaved caspase-9 and cleaved caspase-3 (**Figure 6**), where the induction of cleaved caspase-9 and cleaved caspase-3 occurred at 1.1 - 1.6 times compared to controls, parallel to the previous study where campesterol was shown to be able to induce apoptosis via caspase-9 and caspase-3 proteins in ovarian cancer cells in a dose-dependent manner. The synthesized caspase-9 and caspase-3 proteins have the same expression pattern as the genes encoding these proteins, meaning that all genes were expressed and translated into proteins. The increased expression of caspase-9 and caspase-3 upon activation and during division suggested the intrinsic apoptotic pathway as the mechanism underlying B16-F10 melanoma cell death [40,41].

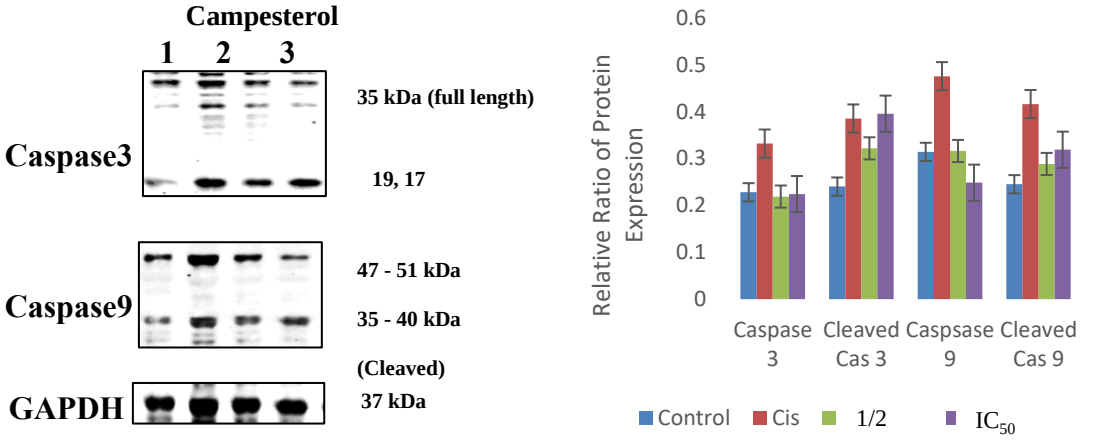

Figure 6 Analysis of protein expression of caspase-9 and caspase-3 in melanoma cells (B16-F10) treated with campesterol. (A) changes in protein expression levels (1: Negative control, 2: Cisplatin control, 3: ½C_{50} 4: IC_{50}), (B) Relative ratio of protein expression of caspase-3, cleaved caspase-3, caspase-9 and cleaved caspase-9.

Conclusions

The findings revealed that 3 well-known steroids, namely *β*-sitosterol (1), Campesterol (2), and Cholesterol (3), were successfully isolated from the *n*-hexane extract of fresh roots of Cassava (*M. esculenta* C.). Notably, Campesterol (2) exhibited the highest IC_{50} value compared to *β*-sitosterol (1) and Cholesterol (3). This indicated that Campesterol (2) significantly impeded the proliferation of B16-F10 cells by inducing apoptosis through caspase 3 activation. These results provided valuable insights into the potential use of Campesterol (2) as a chemopreventive agent for combating melanoma skin cancer.

Acknowledgements

This research received financial support from LPPM Universitas Pakuan (Yayasan Pakuan Siliwangi). We would like to express our gratitude to Erina Hilmayanti for her assistance in the analysis process

References

[1] SP Wooding and CN Payahua. Ethnobotanical diversity of cassava (Manihot esculenta Crantz) in the Peruvian Amazon. *Diversity* 2022; **14**, 252.
[2] SK Muiruri, VO Ntui, L Tripathi and JN Tripathi. Mechanisms and approaches towards enhanced drought tolerance in cassava (*Manihot esculenta*). *Curr. Plant Biol.* 2021; **28**, 100227.
[3] W Shebaby, A Elias, M Mroueh, B Nehme, NDE Jalbout, R Iskandar, JC Daher, M Zgheib, P Ibrahim, V Dwairi, JM Saad, RI Taleb and CF Daher. Himachalol induces apoptosis in B16-F10 murine melanoma cells and protects against skin carcinogenesis. *J. Ethnopharmacol.* 2020; **253**, 112545.
[4] I Boukhers, F Boudard, S Morel, A Servent, K Portet, C Guzman, M Vitou, J Kongolo, A Michel and P Poucheret. Nutrition, healthcare benefits and phytochemical properties of cassava (*Manihot esculenta*) leaves sourced from three countries (Reunion, Guinea, and Costa Rica). *Foods* 2022; **11**, 2027.
[5] M Jampa, K Sutthanut, N Weerapreeyakul, W Tukummee, J Wattanathorn and S Muchimapura. Multiple bioactivities of Manihot esculenta leaves: Uv Filter, anti-oxidation, anti-melanogenesis, collagen synthesis enhancement, and anti-adipogenesis. *Molecules* 2022; **27**, 1556.
[6] D Widiastuti, AH Mulyati, E Herlina, S Warnasih, T Triastinurmiatiningsih and S Unang. Cytotoxic effects of cassava (Manihot esculenta Crantz), Adira-2, karikil and sao pedro petro varieties against P-388 murine leukemia cells. *Res. J. Chem. Environ.* 2018; **22**, 206-8.
[7] D Widiastuti, SE Sinaga, S Warnasih, E Pujiyawati, S Salam and WE Putra. Identification of active compounds from Averrhoa bilimbi L. (Belimbing Wuluh) flower using LC-MS and antidiabetic activity test using in vitro and in silico Approaches. *Trends Sci.* 2023; **20**, 6761.
[8] D Widiastuti, S Salam, D Haneti, R Lesmana, MA Nafiah and U Supratman. Flavonoid from the Sao

Pedro Petro of tubers of cassava (Manihot esculenta Crantz). *Res. J. Chem. Environ.* 2019; **23**, 111-3.

[9] SE Sinaga, FF Abdullah, U Supratman, T Mayanti and R Maharani. Isolation and structure determination of stigmaterol from the stem bark of lansium domesticum Corr. Cv. Kokossan. *Chim. Nat. Acta* 2022; **10**, 106-11.

[10] S Chummun and NR McLean. The management of malignant skin cancers. *Surgery* 2017; **35**, 519-24.

[11] M Potez, V Trappetti, A Bouchet, C Fernandez-Palomo, E Güç, WW Kilarski, R Hlushchuk, J Laissue and V Djonov. Characterization of a B16-F10 melanoma model locally implanted into the ear pinnae of C57BL/6 mice. *PLos One* 2018; **13**, e0206693.

[12] Y Harada, Y Kizuka, Y Tokoro, K Kondo, H Yagi, K Kato, H Inoue, N Taniguchi and I Maruyama. N-glycome inheritance from cells to extracellular vesicles in B16 melanomas. *FEBS Lett.* 2019; **593**, 942-51.

[13] JO Pinho, M Matias, V Marques, C Eleutério, C Fernandes, L Gano, JD Amaral, E Mendes, MJ Perry, JN Moreira, G Storm, AP Francisco, CMP Rodrigues and MM Gaspar. Preclinical validation of a new hybrid molecule loaded in liposomes for melanoma management. *Biomed. Pharmacother.* 2023; **157**, 114021.

[14] T Krajnović, D Drača, GN Kaluđerović, D Dunđerović, I Mirkov, LA Wessjohann, D Maksimović-Ivanić and S Mijatović. The hop-derived prenylflavonoid isoxanthohumol inhibits the formation of lung metastasis in B16-F10 murine melanoma model. *Food Chem. Toxicol.* 2019; **129**, 257-68.

[15] JM Estrela, R Salvador, P Marchio, SL Valles, R López-Blanch, P Rivera, M Benlloch, J Alcácer, CL Pérez, JA Pellicer and E Obrador. Glucocorticoid receptor antagonism overcomes resistance to BRAF inhibition in BRAFV600E-mutated metastatic melanoma. *Am. J. Canc. Res.* 2019; **9**, 2580-98.

[16] GK Couto, NV Segatto, TL Oliveira, FK Seixas, KM Schachtschneider and T Collares. The melding of drug screening platforms for melanoma. *Front. Oncol.* 2019; **9**, 512.

[17] T Komel, M Bosnjak, SK Brezar, MD Robertis, M Mastrodonato, G Scillitani, G Pesole, E Signori, G Sersa and M Cemazar. Gene electrotransfer of IL-2 and IL-12 plasmids effectively eradicated murine B16.F10 melanoma. *Bioelectrochemistry* 2021; **141**, 107843.

[18] F Mirzavi, M Barati, A Soleimani, R Vakili-Ghartavol, MR Jaafari and M Soukhtanloo. A review on liposome-based therapeutic approaches against malignant melanoma. *Int. J. Pharm.* 2021; **599**, 120413.

[19] SE Sinaga, M Fajar, T Mayanti and U Supratman. Bioactivities screening and elucidation of terpenoid from the stembark extracts of lansium domesticum Corr. cv. Kokosan (Meliaceae). *Sustainability* 2023; **15**, 2140.

[20] D Widiastuti, S Salam, D Haneti and RLU Supratman. Cytitoxic activity from the tuber of cassava (*Manihot esculenta* crantz) against servical hela cancer lines. *Int. J. Recent Tech. Eng.* 2019; **8**, 243-4.

[21] Y Bodurlar and M Caliskan. Inhibitory activity of soybean (*Glycine max* L. Merr.) cell culture extract on tyrosinase activity and melanin formation in alpha-melanocyte stimulating hormone-induced B16-F10 melanoma cells. *Mol. Biol. Rep.* 2022; **49**, 7827-36.

[22] HJ Han, SK Park, JY Kang, JM Kim, SK Yoo and HJ Heo. Anti-melanogenic effect of ethanolic extract of sorghum bicolor on IBMX-induced melanogenesis in B16/F10 melanoma cells. *Nutrients* 2020; **12**, 832.

[23] S Susianti, R Lesmana, S Salam, E Julaeha, YS Pratiwi, N Sylviana, H Goenawan, A Kurniawan and U Supratman. The effect of nutmeg seed (*M. fragrans*) extracts induces apoptosis in melanoma maligna cell's (B16-F10). *Indonesian Biomed. J.* 2021; **13**, 68-74.

[24] T Kim, KB Kim and CG Hyun. A 7-Hydroxy 4-methylcoumarin enhances melanogenesis in b16-f10 melanoma cells. *Molecules* 2023; **28**, 3039.

[25] EK Sutedja, D Amarassaphira, H Goenawan, YS Pratiwi, N Sylviana, B Setiabudiawan, O Suwarsa, RTD Judistiani, U Supratman and R Lesmana. Calcitriol inhibits proliferation and potentially induces apoptosis in B16-F10 cells. *Med. Sci. Mon. Basic Res.* 2022, **28**, e935139.

[26] CC Jan-Michael and CY Ragasa. Structure elucidation of β-stigmasterol and β-sitosterol from Sesbania grandifora [Linn.] Pers. and β-carotene from Heliotropium indicum Linn. by NMR spectroscopy. *Kimika* 2004; **20**, 5-12.

[27] E Hadrian, AP Sari, T Mayanti, D Harneti, R Maharani, D Darwati, K Farabi, U Supratman, C Waranmaselembun and S Salam. Steroids from *Atactodea striata* and their cytotoxic activity against MCF-7 Breast Cancer Cell Lines. *Indonesian J. Chem.* 2022; **23**, 200-9.

[28] MY Morad, H El-Sayed, MF El-Khadragy, A Abdelsalam, EZ Ahmed and AM Ibrahim. Metabolomic profiling, antibacterial, and molluscicidal properties of the medicinal plants *Calotropis procera* and *Atriplex halimus: In silico* molecular docking study. *Plants* 2023; **12**, 477.
[29] S Nikita, K Thakur, A Chhokar, J Yadavi, T Tripathi, Jadli, M Bhat, Anjali, A Kumar, RH Narula, R Hasija, G Pankaj, A Khurana, A Bharti and TA Chandra. Evaluation of therapeutic potential of selected plant-derived homeopathic medicines for their action against cervical cancer. *Homeopathy* 2023; **112**, 262-74.
[30] S Pathania, P Bansal, P Gupta and RK Rawal. Genus calotropis: A hub of medicinally active phytoconstituents. *Curr. Tradit. Med.* 2019; **6**, 312-31.
[31] RK Saini, YS Keum, M Daglia and KR Rengasam. Dietary carotenoids in cancer chemoprevention and chemotherapy: A review of emerging evidence. *Pharmacol. Res.* 2020; **157**, 104830.
[32] MI Rushdi, IAM Abdel-Rahman, EZ Attia, H Saber, AA Saber, G Bringmann and UR Abdelmohsen. The biodiversity of the genus dictyota: Phytochemical and pharmacological natural products prospectives. *Molecules* 2022; **27**, 672.
[33] J Wu, J Ye, W Kong, S Zhang and Y Zheng. Programmed cell death pathways in hearing loss: A review of apoptosis, autophagy and programmed necrosis. *Cell Prolif.* 2020; **53**, e12915.
[34] M Jiang, L Qi, L Li and Y Li. The caspase-3/GSDME signal pathway as a switch between apoptosis and pyroptosis in cancer. *Cell Death Discov.* 2020; **28**, 112.
[35] S Umar, R Soni, SD Durgapal, S Soman and S Balakrishnan. A synthetic coumarin derivative (4 - flourophenylacetamide - acetyl coumarin) impedes cell cycle at G0/G1 stage , induces apoptosis, and inhibits metastasis via ROS - mediated p53 and AKT signaling pathways in A549 cells. *J. Biochem. Mol. Toxicol.* 2020; **34**, e22553.
[36] V Singh, A Khurana, U Navik, P Allawadhi, KK Bharani and R Weiskirchen. Apoptosis and pharmacological therapies for targeting thereof for cancer therapeutics. *Sci* 2022; **4**, 15.
[37] M Hadzic, Y Sun, N Tomic and E Tsirvouli, M Kuiper and L Pojskic. Halogenated boroxine increases propensity to apoptosis in leukemia (UT-7) but not non-tumor cells *in vitro. FEBS Open Bio* 2023; **13**, 143-53.
[38] K Fettucciari, F Marguerie, A Fruganti, A Marchegiani and A Spaterna, S Brancorsini, P Marconi and G Bassotti. Clostridioides difficile toxin B alone and with pro - inflammatory cytokines induces apoptosis in enteric glial cells by activating three different signalling pathways mediated by caspases, calpains and cathepsin B. *Cell. Mol. Life Sci.* 2022; **79**, 442.
[39] WE Yang, YT Chen, CW Su, MK Chen, CM Yeh, YL Chen, MY Tsai, SF Yang and CW Lin. Hispolon induces apoptosis in oral squamous cell carcinoma cells through JNK/HO-1 pathway activation. *J. Cell. Mol. Med.* 2023; **27**, 1250-60.
[40] LE Araya, IV Soni, JA Hardy and O Julien. Deorphanizing caspase-3 and caspase-9 substrates in and out of apoptosis with deep substrate profiling. *ACS Chem. Biol.* 2022; **16**, 2280-96.
[41] MA Wride, FC Mansergh, S Adams, R Everitt, SE Minnema, E Rancourt and MJ Evans. Expression profiling and gene discovery in the mouse lens. *Mol. Vis.* 2003; **22**, 360-96